Immunity, Vol. 10, 577–584, May, 1999, Copyright ©1999 by Cell Press

Crystal Structure of the MHC Class I Homolog MIC-A, a γδ T Cell Ligand

Pingwei Li,* Sirkku T. Willie,* Stefan Bauer,† Daniel L. Morris,* Thomas Spies,† and Roland K. Strong*‡

*Division of Basic Science

†Division of Clinical Research

Fred Hutchinson Cancer Research Center

Seattle, Washington 98109

Summary

The major histocompatibility complex (MHC) class I homolog MIC-A functions as a stress-inducible antigen that is recognized by a subset of γδ T cells independent of β_2-microglobulin and bound peptides. Its crystal structure reveals a dramatically altered MHC class I fold, both in detail and overall domain organization. The only remnant of a peptide-binding groove is a small cavity formed as the result of disordering a large section of one of the groove-defining helices. Loss of β_2-microglobulin binding is due to a restructuring of the interaction interfaces. Structural mapping of sequence variation suggests potential receptor binding sites on the underside of the platform on the side opposite of the surface recognized by αβ T cell receptors on MHC class I–peptide complexes.

Introduction

Responses by cellular components of the adaptive immune system involve the specific recognition of antigen-derived peptides bound to major histocompatibility complex (MHC) proteins by αβ T cell receptors (TCRs) (Germain and Margulies, 1993; Rock, 1996). A second class of T cells, those bearing γδ TCRs, are proposed to mediate antimicrobial responses and regulate innate and acquired immunity (Allison and Raulet, 1990; Porcelli et al., 1991; Kaufmann, 1996). The rules governing the interactions between γδ TCRs and their ligands are believed to be distinct from those directing the interaction between αβ TCRs and their ligands (Chien and Jores, 1995; Chien et al., 1996). One subset of γδ T cells, those expressing $V_\delta1$ TCRs, broadly recognize the distant MHC class I homologs MIC-A and MIC-B (Bahram and Spies, 1996; Bahram et al., 1994, 1996; Groh et al., 1996, 1998). Unlike conventional MHC class I proteins, MIC-A requires neither peptide nor β_2-microglobulin (β_2-m) for stability or cell-surface expression (Groh et al., 1996). We report the crystal structure of a soluble fragment of human MIC-A in order to provide a structural context for understanding γδ T cell–mediated antigen recognition.

The "classical" or class Ia MHC proteins (HLA-A, -B, and -C) are integral-membrane, heterodimeric proteins (Bjorkman and Parham, 1990). The heavy chain of these proteins comprises three extracellular domains (α1, α2, and α3), a transmembrane-spanning domain, and a small cytoplasmic domain; the light-chain is β_2-m. In MHC class I proteins, the α1 and α2 domains, defined on the basis of internal sequence homology, together comprise the peptide- and TCR-binding "platform" domain. The MHC class Ia molecules are polymorphic and ubiquitously expressed. The sequence polymorphism reflects the ability of these proteins to bind to a variety of peptide ligands and TCRs (Rammensee et al., 1993a, 1993b; Davis et al., 1998). MIC-A and MIC-B, conserved in most mammals except rodents, are homologous to MHC class I proteins. Unlike MHC class Ia proteins, however, the expression of MIC proteins is essentially restricted to gut epithelium, and the corresponding genes appear to be under the control of heat-shock promoter elements (Groh et al., 1996). While MIC-A and MIC-B proteins are quite similar to each other (84% identical [Bahram and Spies, 1996; Bahram et al., 1996]), they have diverged significantly from the MHC class I family as a whole, with identities of 28%, 23%, and 35% in the α1, α2 and α3 domains, respectively, when aligned with the human MHC class I protein HLA-B27.

A variety of nonMHC encoded structural homologs of MHC class I proteins with diverse functions have been identified, thus demonstrating the versatility of the MHC class I fold. CD1 is a family of nonpolymorphic, cell-surface glycoproteins that while not encoded within the MHC, present mycobacterial cell wall antigens (such as mycolic acid and lipoarabinomannans) to some T cells (Porcelli et al., 1998). The structure of CD1 reveals a binding groove dramatically altered to accommodate these nonpeptide ligands (Zeng et al., 1997). The neonatal rat Fc receptor (FcRn) mediates the transport of maternal IgG from the gut of a nursing neonate to its bloodstream (Simister and Rees, 1985). The interaction with IgG is through a surface distinct from the TCR footprint on MHC class I proteins (Burmeister et al., 1994a, 1994b). FcRn does not bind peptides. HFE, the protein associated with hereditary hemochromatosis, binds to transferrin receptor but not to peptides (Feder et al., 1998). Again, this interaction is likely different from those class I proteins make with TCR or CD8 (Lebrón et al., 1998). The structure of serum Zn-α_2-glycoprotein (ZAG), which like MIC-A neither binds peptides nor β_2-m, has recently been determined (Sanchez et al., 1999). Cytomegalovirus also encodes an MHC class I homolog, UL18, which is proposed to bind NK cell killer inhibitory receptors, though its structure remains undetermined (Fahnestock et al., 1995; Cosman et al., 1997).

Results and Discussion

Architecture

The crystal structure of the extracellular region of human MIC-A (allele 001, residues 1–274 plus a His_6 purification tag) was determined at 2.8 Å resolution by multiple isomorphous replacement (Table 1 and Figure 1A). As with the heavy chains of peptide-binding MHC class I proteins and non-peptide-binding homologs, the structure

‡To whom correspondence should be addressed (e-mail: rstrong@fhcrc.org).

Table 1. Data Collection and Refinement Statistics

Data Collection

Data Set	Native(1)	Native(2)	$NaAuCl_4$(1)	$NaAuCl_4$(2)	K_2HgI_4	K_2PtCl_4	K_2OsO_4(1)	K_2OsO_4(2)
Resolution (Å)	3.2	2.8	4.0	3.8	4.0	4.5	4.0	4.0
Observations	61794	130489	34903	38323	31022	13582	20246	30905
Unique Reflections	12911	19368	6658	7210	6666	4274	6022	5407
Completeness (%)	98.2(89.8)	99.7(100)	99.0(97.0)	92.6(95.8)	97.2(99.1)	89.3(89.7)	89.0(91.2)	79.6(79.1)
I/σI	15.0(3.3)	42.0(5.8)	14.4(3.3)	23.9(4.9)	21.4(4.3)	21.1(3.7)	13.8(3.1)	17.6(3.1)
R_{sym} (%)	13.2(39.6)	6.3(32.9)	11.7(39.7)	9.1(33.6)	10.8(31.6)	8.5(24.3)	9.5(37.7)	10.8(43.3)
Number of Sites	—	—	2	2	4	1	1	1
Isomorphous Difference (%)	—	—	23.7	29.8	27.4	31.0	22.3	36.5
Phasing Power	—	—	1.38	1.59	1.05	1.18	0.71	1.03
R_{cullis} (%)	—	—	0.72	0.68	0.91	0.86	0.90	0.86

Refinement Statistics

Resolution (Å)	Reflections ($F > 0$)	Protein Atoms	Solvent Atoms	CHO Atoms	R_{Cryst}/R_{Free} (%)
∞–2.8	18416	2117	19	28	25.3/29.3

	Quality of the Model (RMSD)			Ramachandran Plot	
Bond Length	Bond Angles	Dihedrals	Average B Factor	Most Favored	Disallowed
0.014Å	1.9°	26.9°	46.13 $Å^2$	81.9%	0

Values for the highest resolution shell are shown in parentheses.

$R_{sym} \equiv \Sigma|I - <I>|/\Sigma<I>$ where I is the observed intensity and $<I>$ is the mean intensity of multiple observations of symmetry-related reflections.

Phasing Power $\equiv <|F_H|>/E$ where F_H is the heavy atom structure factor amplitude and E is the residual lack-of-closure error.

$R_{cullis} \equiv \Sigma|F_{PH} - F_P| - |F_{H(calc)}|/\Sigma|F_{PH} - F_P|$ where F_P is the protein structure factor amplitude and F_{PH} is the heavy atom derivative structure factor amplitude.

R_{Cryst}, $R_{Free} \equiv \Sigma\ ||F_{obs}| - |F_{calc}||/\Sigma|F_{obs}|$ where F_{obs} and F_{calc} are observed and calculated structure factor amplitudes, respectively. R_{free} is calculated for a randomly chosen 10% of the reflections excluded from refinement (Brünger, 1992).

of MIC-A consists of two structural domains: platform ($\alpha1\alpha2$) and $\alpha3$. The platform domain of MHC class I proteins comprises two long, roughly parallel α helices, interrupted by bends, arranged on an eight-stranded β sheet. The individual helical elements are labeled 1 and 2 in the $\alpha1$ domain and 1, 2a, and 2b in the $\alpha2$ domain (see Figure 2). These α helices define the peptide binding groove in MHC class I homologs that bind peptides. In MIC-A, the pseudo 2-fold symmetric platform consists of four distinct α helices arranged on an eight-stranded anti-parallel β sheet. As shown in Figure 2, these helices are labeled 1 and 2 in the $\alpha1$ domain and 1 and 2b in the $\alpha2$ domain (secondary structure elements are numbered using the HLA-B27 nomenclature). Helix 1 in the $\alpha1$ domain of MIC-A is longer and much more clearly delineated from helix 2 than its counterpart in other MHC class I homologs, and it is therefore better described as a separate helix rather than as a segment of a longer helix. Likewise, helix 1 and 2b in the $\alpha2$ domain are clearly distinct elements.

In MIC-A, no electron density is observed for ten residues (152–161) in one section of these helices (corresponding to helix 2a in the $\alpha2$ domain of HLA-B27) or for the polyhistidine purification tag. These residues are therefore presumed to comprise conformationally ill-defined loops extending into solvent, at least under the crystallization conditions (pH 5.5). Five residues (147–151) next to the disordered loop have been modeled as alanines due to the lower quality of the electron density in this region. Preliminary results from limited proteolysis with thermolysin at pH 7.5, in which MIC-A is initially cleaved in the region of this loop, suggest that this loop is exposed and flexible at near neutral pH as well (data not shown). The sequence of the residues in this loop are highly conserved (only two single substitutions observed in 16 human MIC-A alleles) (Fodil et al., 1996). The result of remodeling helix 2a in the $\alpha2$ domain is a gap or pocket in the otherwise smooth surface of the MIC-A platform (Figures 3A and 3C). This fairly small pocket (roughly 12 × 10 × 7 Å) is predominantly lined with hydrophilic residues: Asn-69, Asp-72, Glu-92, Arg-94, Gln-108, Gln-120, and Leu-122. Other than this pocket, there are no other remnants of a peptide-binding groove unlike other class I homologs, i.e., FcRn, which retains a small gap in place of the groove (Figure 3C) (Burmeister et al., 1994a). The boundaries of the disordered loop in MIC-A precisely coincide with discontinuities in the helical secondary structure that delineate helices 1, 2a, and 2b in the $\alpha2$ domains of all other class I MHC homologs (Figure 2).

The structural homology between the MIC-A platform and the platforms of other MHC class I homologs is strongest for the six central strands of the β sheet (see Figure 3B). When all eight strands of the β sheet are considered, significant differences appear between MIC-A and the non–class Ia molecules, but the homology to the class Ia proteins is still remarkable. Structural differences between MIC-A and the class I homologs accumulate when the entire platform is compared, particularly in the loop between the first two strands of the β sheet (residues 13–20) and the hairpin connecting the third and fourth β strands (residues 37–40) (Figure 3B). Helix 1 in the $\alpha1$ domain (residues 45–54) is much longer than any other class I homolog. Overall, the fold of the $\alpha2$ domain of MIC-A is most similar to that of FcRn.

The lack of any remnant of a peptide-binding groove

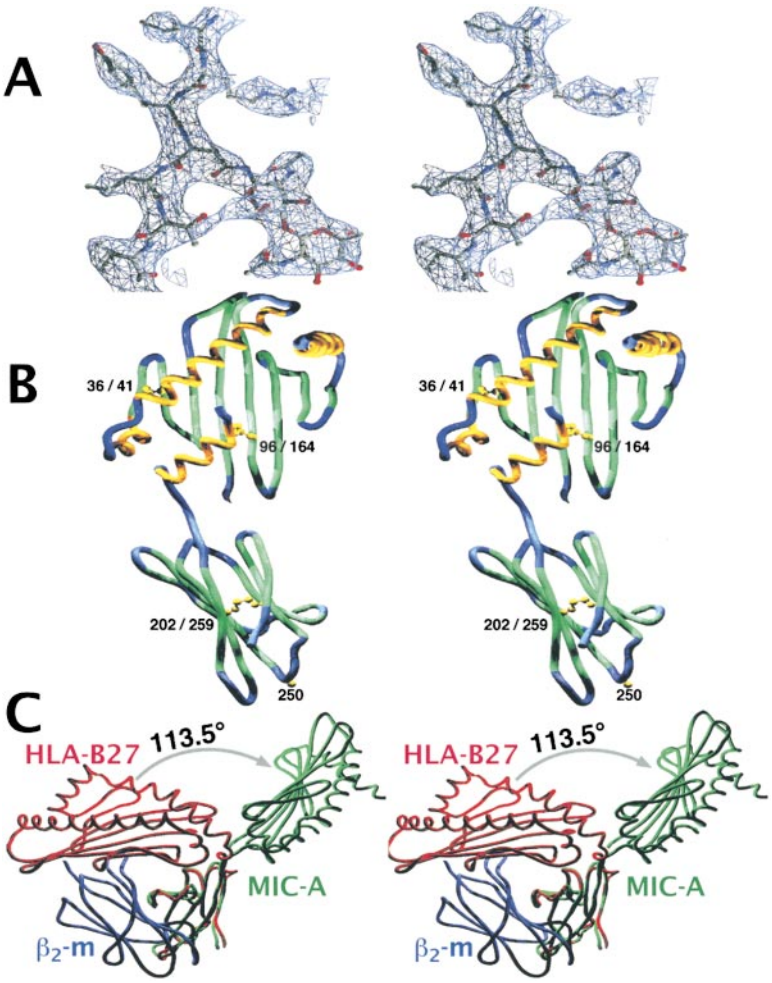

Figure 1. The Overall Structure of MIC-A

(A) Stereoview of the 3.2 Å resolution solvent-flattened experimental electron density map (blue net) in the vicinity of Asn-8, contoured at 1.25σ and superimposed on residues from the final model. Atoms are colored as follows: gray, carbon; red, oxygen; and blue, nitrogen.

(B) Stereoview of a ribbon representation of the fold of MIC-A. Secondary structure is colored as follows: yellow, α helix; green, β strand; and blue, coil. Cysteine side chains are numbered and shown in ball-and-stick representation.

(C) Stereoview of the superposition of the α3 domain of MIC-A onto that of HLA-B27. The chains are colored as follows: green, MIC-A; blue, HLA-B27 heavy chain (platform and α3 domains); and red, β_2-m. The root mean square deviation (RMSD) between 80 comparable Cαs in the α3 domains of MIC-A and HLA-B27 is 0.74 Å, and it is 1.17 Å for the 81 comparable Cαs in the α3 domains of MIC-A and β_2-m. Figures were generated with Swiss-PDBViewer and rendered with POV-RAY3.

results in part from a significant narrowing of the gap between the groove-defining helices to approximately 10 Å between the helices (Cα to Cα) over the first four strands of the β sheet and 7 Å between the helices over the second four strands of the β sheet. Side chains of several residues also overlay the region where a gap might open (Figure 3A). The close approach of the helices at the conserved disulfide (96/164) is facilitated by a structure we term the "latch" (Figure 4A). The conformation of this disulfide bond is conserved in all class I homologs and is facilitated by conservation of a glycine (Gly-100 in HLA-B27) neighboring the first cysteine. A glycine at this position (the latch residue) allows the backbone to pucker upward toward the helix out of the plane of the β sheet, adopting ϕ/ψ angles disallowed for nonglycine amino acids. The ϕ/ψ values for the conserved glycine in HLA-B27, CD1, and FcRn range from ϕ: 159° to 173° and ψ: −161° to -172°. This glycine is replaced by a valine (Val-95) in MIC-A, straightening the backbone into the plane of the β sheet: $\phi = -122°/\psi = 161°$. The resulting tug changes the disulfide bridge from left-handed in all other class I homologs to right-handed in MIC-A and shifts the axis of the helix by almost 3 Å, narrowing the groove. This valine is conserved in all human MIC sequences (Fodil et al., 1996) and is replaced with isoleucine, leucine, or asparagine in some of the nonhuman primate MIC sequences (Steinle et al., 1998).

The α3 domain of MIC-A adopts a C-type immunoglobulin fold very similar in structure to the α3 domains of MHC class I proteins and homologs, as well as β_2-m itself. The relative orientation of the two domains in MIC-A is dramatically different from that of all other MHC class I proteins and related molecules and results in an extended structure with two distinct domains (Figures 1C and 4). The linker between the platform and α3 domains in MIC-A consists of four residues (Leu-178 to Thr-181) in an extended conformation, unlike the additional turn of helix found in the linkers of other MHC class I homologs. There are no contacts between the two domains, and the linker is sufficient to allow for considerable interdomain flexibility. The electron density for the entire backbone of MIC-A including this linker, with the exception of the disordered loop and His-tag, is clear, unambiguous, and readily traceable in the initial, experimental maps. This suggests that our structure represents a single interdomain conformation of an otherwise flexibly linked molecule selected by extensive crystal contacts (see below).

There are eight N-linked glycosylation sites in MIC-A001 that are fully utilized in protein isolated from human cells as determined by partial digestion with endoglycosidase H (data not shown). In the crystal structure, there is well-defined electron density for two N-acetyl glucosamine (NAG) residues at Asn-8, which have been

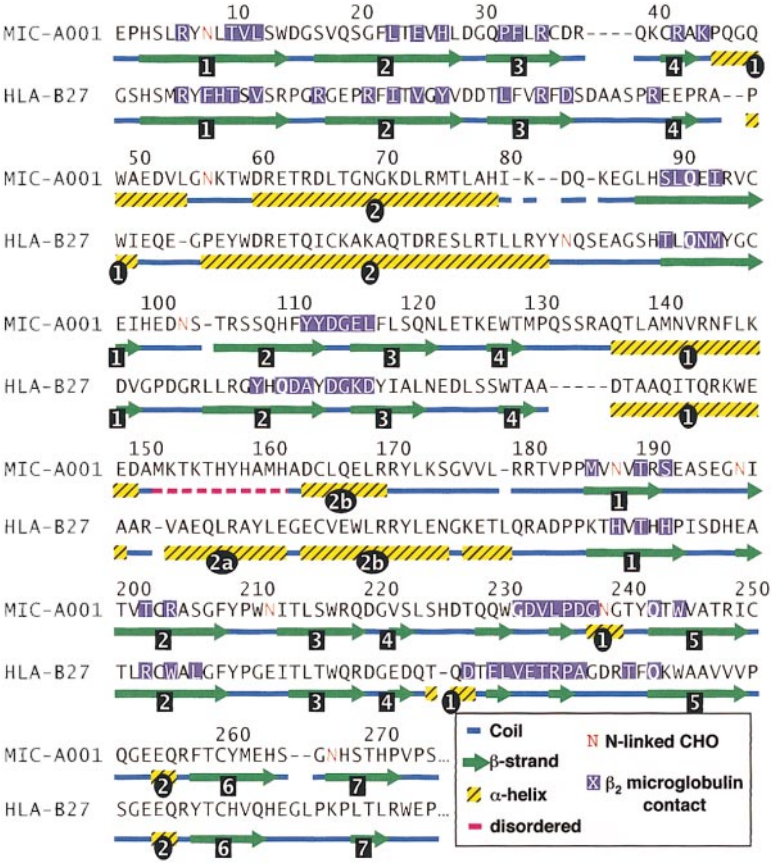

Figure 2. Manual, Structure-Based Alignment of the Sequences of Human MIC-A001 and HLA-B27

MIC-A residues are numbered sequentially from the N terminus. This alignment differs significantly from prior published alignments. Beneath each sequence is shown the corresponding secondary structure elements (numbered as in HLA structures) colored as indicated. Helices are numbered in ovals; strands are numbered in squares. The sequence-defined domains α1, α2, and α3 comprise residues 1–85, 86–178, and 182–276, respectively. Residues 179, 180, and 181 form a short linker between the platform and α3 domains in MIC-A. Gaps introduced to account for insertions in one sequence relative to the other are indicated by dashes. Potential N-linked oligosaccharide sites are shown in red. Residues with solvent accessible surface area buried by β_2-m are shown outlined in purple. For MIC-A, these residues were determined by positioning β_2-m against the MIC-A platform and α3 domains separately, based on superpositions of these domains with the corresponding domains of HLA-B27.

included in the model (Figure 1A). There is less well-defined density at Asn-102, Asn-187, Asn-211, Asn-238, and Asn-266 that likely corresponds to carbohydrate, but which we have not been able to confidently model as such. We see no evidence for N-linked carbohydrate at Asn-56 or Asn-197 in the current electron density map. The asparagine side chains at all eight sites are accessible. Beyond the disulfide bridges conserved in all MHC class I family members (cysteines 96/164 and cysteines 202/259 in MIC-A), there is an extra disulfide bridge between Cys-35 and Cys-40 closing off a loop of four residues.

Crystal Packing Interactions

The soluble, recombinant MIC-A is monomeric and monodisperse in solution over a pH range of 5.5 to 7.4 (data not shown). However, a particularly intimate interaction is seen in the MIC-A crystals. In a tight dimer, the α3 domain of one monomer reciprocally binds to the platform domain of the dyad-related monomer (Figures 4A and 4B). The Asn-8 oligosaccharide makes contacts to the dyad-related α3 domain, likely explaining why these NAGs are ordered in our structure. In this dimer, the position of the α3 domain is related by an approximate dyad axis of symmetry through Asn-8 to the position of β_2-m in a MHC class I protein. The accessible surface area buried on the platform (532 Å^2) and on α3 (586 Å^2) by this association is comparable to the area buried by β_2-m in class I proteins. However, this dimer cannot form on the cell surface, as the shortest distance from the C-termini in the dimer to a membrane would be from 13 to 15 Å, a distance too long to be spanned by the two residues unaccounted for in our structure. This dimer, however, does demonstrate that the Asn-8 oligosaccharide does not completely block protein–protein interactions on the underside of the platform.

Lack of β_2-Microglobulin Binding

The β_2-m binding interfaces are oriented in incompatible directions in the extended structure of MIC-A present in the crystal (Figures 5A and 5B). However, the interdomain flexibility is likely sufficient to allow MIC-A to adopt a classical heavy chain conformation. Thus, we conclude that the observed interdomain orientation in MIC-A does not contribute to the lack of β_2-m binding. The N-linked oligosaccharide site at Asn-8 is situated near the center of the β_2-m binding surface on the underside of the platform (Figures 5A and 5B) and would preclude β_2-m binding when present, as with our recombinant protein. The two NAGs overlap with Phe-56 and Phe-62 of β_2-m when MIC-A is superimposed on class I structures. This glycosylation site is conserved in all primate MIC sequences except in human MIC-B, so this clash cannot solely account for loss of β_2-m binding across the MIC family. No other N-linked glycosylation site either observed in our structure or possibly present in any other MIC sequence obviously interferes with β_2-m binding (Figures 5A and 5B).

The core of the β_2-m–platform interface in MHC class

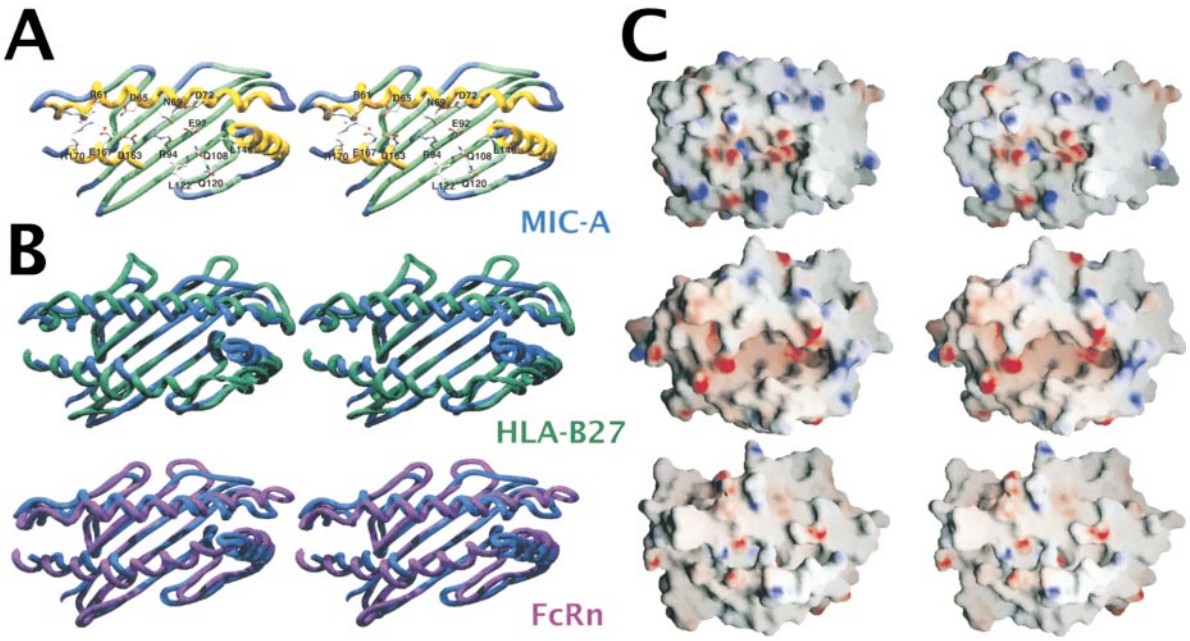

Figure 3. Comparisons of the Platforms of MIC-A and Other MHC Class I Proteins

(A) Stereoview of the platform domain of MIC-A showing the side chains of residues with appreciable solvent accessibility near the region of the peptide-binding groove present in other MHC class I structures. Features are colored as in Figure 1.

(B) Stereoviews of superpositions of the structures of the platform domains of MIC-A (blue), HLA-B27 (green), MIC-A (blue), and FcRn (purple). When only the six central β strands of the platform domains are considered, the RMSD is 1.05 Å for MIC-A compared to HLA-B27 (Protein Data Bank file 1hsa.pdb, calculated on alignment of 46 Cαs), 1.12 Å for MIC-A and CD1 (file 1cd1.pdb, 49 Cαs aligned) and 1.23 Å for MIC-A and FcRn (file 1fru.pdb, 46 Cαs aligned). When all eight strands of the β sheet are considered, the RMSD increases to 1.29 Å in an alignment of 63 Cαs in MIC-A and HLA-B27. The RMSD for the alignment of the α2 domains of MIC-A and FcRn is 1.82 Å, based on 95 Cαs.

(C) GRASP (Nicholls et al., 1991) molecular surfaces, colored by electrostatic potential (blue, positive; red, negative) for MIC-A (top), HLA-B27 (middle), and FcRn (bottom).

I molecules, CD1, and FcRn is formed by four residues in β_2-m (His-31, Phe-56, Trp-60, and Phe-62) that cluster around a glutamine (Gln-96 in HLA-B27) that is one of three conserved residues (Gln-96, Ala-117, and Gly-120, numbered as in HLA-B27) at this interface. In MIC-A, the residues corresponding to these conserved residues are also conserved except for Tyr-111, which corresponds to Ala-117 in HLA-B27. The side chain of Tyr-111 sterically clashes with Trp-60 of β_2-m when MIC-A is superimposed onto a class I structure, occluding β_2-m binding. The Tyr-111 substitution is uniformly conserved in all primate MIC sequences (Fodil et al., 1996; Steinle et al., 1998). Glu-25 and Arg-35 in MIC-A form a salt bridge that would sterically clash with Glu-53 and Ser-55 of β_2-m. These two residues are also conserved in all human and most primate MIC sequences. An aspartic acid residue conserved in class Ia molecules (Asp-122 in HLA-B27) forms a hydrogen bond with Trp-60 of β_2-m. This residue is replaced by either leucine (residue 116) in most primate MIC sequences or an arginine in some of the Old World monkey alleles. Either substitution ablates this favorable interaction. There are no obvious steric clashes between any MIC-A α3 domain residues and β_2-m when MIC-A is docked onto a class I structure, but the overall character of the contact surface is quite different (Figure 2). However, the β_2-m–α3 interaction contributes little to binding in class I MHC proteins as demonstrated by the dissociation of α3 when the platform/α3 linker is severed (Collins et al., 1995).

The sum of these interactions likely explains the lack of β_2-m binding by MIC-A but does not explain how MIC-A stably folds in the absence of β_2-m association. ZAG, which also does not bind β_2-m, is stabilized by extending the contact surface between the platform and α3 domains (Sanchez et al., 1999). This mechanism is not utilized by MIC-A, as there are no interactions between platform and α3. The large number of N-linked oligosaccharides present on the molecule may provide enhanced stability, but examination of the structure reveals no other immediately apparent explanation.

Structural Implications for Ligand Binding

The uniform cytolytic response of diverse human $V_\delta1^+$ γδ cell clones against target cells expressing various divergent human or nonhuman primate MIC proteins demonstrates the promiscuous nature of this interaction (Groh et al., 1998; Steinle et al., 1998). These results suggest the presence of a single, conserved recognition site on MIC proteins. This interpretation contrasts the situation with class I proteins, where sequence *variations* map to peptide and TCR binding sites (Bjorkman and Parham, 1990). Unlike MHC class I proteins and homologs, the surfaces of both domains are completely accessible to solvent or other molecules. In order to define a potential receptor recognition site, the observed allele and species differences between the available MIC sequences were mapped onto the model (Figures 5C and 5D). Prior results had already eliminated the α3 domain from consideration (Groh et al., 1998).

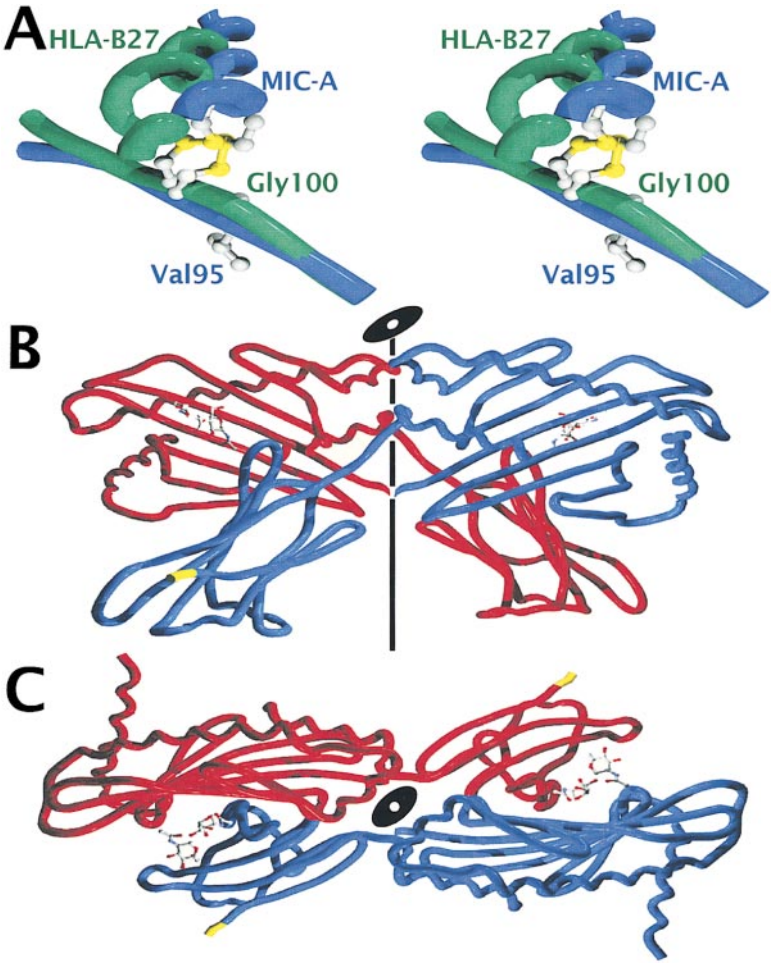

Figure 4. Detailed Views of the "Latch" and the Crystallographic Dimer

(A) Stereoview of a ribbon representation of the folds of MIC-A (blue) and HLA-B27 (green) in the region of helix 2b in the α2 domain highlighting the "latch." The side chains of the latch residue (Val-95 in MIC-A and Gly-100 in HLA-B27) and the conserved disulfide bond (Cys-96/Cys-164) are shown in ball-and-stick representation.

(B and C) A view from the side (B) and from the top (C) of the crystallographic dimer. The two MIC-A monomers, one in red and the other in blue, are shown as backbone ribbons. The ordered N-linked carbohydrate is shown in ball-and-stick representation, and the crystallographic dyad axis is indicated by the black oval. The C-termini of the two monomers are colored yellow.

Most of the conserved residues are found in the hydrophobic cores of the platform and α3 domains. The "top" surface of the MIC-A platform, the surface associated with TCR and peptide binding in MHC class I proteins, is strikingly variable, while the "underside" of the platform, the surface associated with β_2-m binding, shows a marked degree of conservation (or conservative substitution) among these sequences. This conserved surface consists of two "patches" that straddle the conserved glycosylation site at Asn-8 (Figures 5C and 5D). Patch 2 shares a greater area with the β_2-m footprint on class I MHC molecules, while patch 1 defines an area similar to that buried in the crystallographic dimer. We propose that these patches represent potential receptor interaction surfaces.

Conclusions

The crystal structure of MIC-A, while immediately recognizable as a member of the MHC class I structural family, is one of the most distorted examples thus far identified, likely reflecting the distant sequence relationship of MIC-A to other MHC class I homologs. In the platform domain, the most striking change is the disordering of a section of residues that comprise helix 2a in the α2 domains of other MHC class I homologs. Our interpretation is that these residues loop out from the rest of the platform structure and are free to move about in solution, creating a shallow pocket on the surface of the domain under this mobile loop. While we cannot rule out that this pocket represents a binding site for some unidentified nonpeptide ligand, we do not see any density in this region that is not accounted for by protein or ordered solvent. It is possible that under more physiological conditions the unobserved section of this helix becomes ordered, partially or completely filling this pocket, or that it coalesces around some hypothetical small-molecule ligand. All other traces of a conventional peptide-binding groove are absent, partly due to a repositioning of helix 2b in the α2 domain in response to the replacement of a glycine residue conserved in all other class I homologs (the latch residue). Unlike other MHC class I homologs, the platform and α3 domains do not interact except through a short linker peptide that likely allows for considerable flexibility. Intimate intermolecular interactions in the crystal stabilize one particular conformation, allowing the structure to be clearly elucidated. Differences between primate MIC sequences define patterns of conservation on the surface of the structure distinct from the polymorphic surfaces of MHC class I proteins. We propose that two patches of conserved residues on the underside of the platform domain, a surface that is inaccessible in all β_2-m binding MHC class I homologs, may serve as binding sites for receptors that interact with MIC-A.

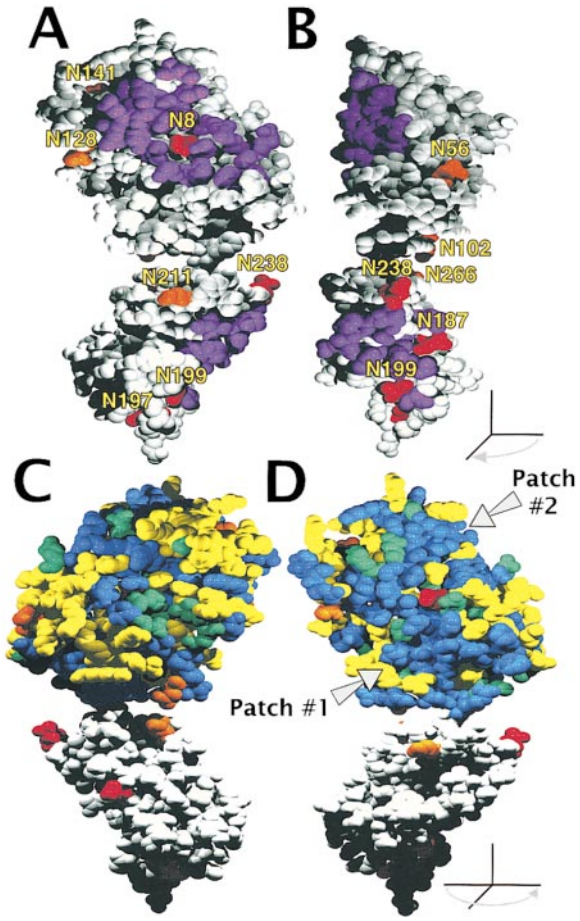

Figure 5. Space-Filling Representations of the Surface Character of MIC-A

(A and B) A view of the back (A) and the side (B) of MIC-A highlighting the potential N-linked oligosaccharide sites present in all primate MIC alleles (orange) and those conserved in all primate MIC-A alleles (red). Residues shown in purple correspond to residues buried in a hypothetical complex with β_2-m (see Figure 3).

(C and D) Views of the equivalent of the peptide/TCR-binding surface of the platform domain (the "top," [C]) and the β_2-m binding surface of the platform domain (the "underside," [D]; same orientation as in [A]) of MIC-A. Residues conserved across all primate MIC sequences are colored blue; residues where conservative substitutions have occurred (L/V/I, E/D, D/N, E/Q, E/N, or R/K) are colored green; nonconserved residues are colored yellow; residues in the α3 domain are colored gray. Two patches of conserved residues straddle the N-linked oligosaccharide at Asn-8: patch 1 (below Asn-8 in [D]): Ser-4, Arg-6, Glu-25, His-27, Gly-30, Gln-31, Pro-45, Trp-49, Glu-97, and Arg-180; patch 2 (above and to the left of Asn-8 in [D]); Leu-12, Lys-84, Leu-87, His-109, Tyr-111, Asp-113, Gly-114, Glu-115, Gln-131, and Ser-132. Residues at potential N-linked glycosylation sites are colored as in (A) and (B).

Experimental Procedures

Solution Characterization

MIC-A (at 2.0 mg/ml) was digested with thermolysin (Boerhinger-Mannheim) at a ratio of between 50:1 and 25:1 in 50 mM sodium phosphate (pH 7.5) and 150 mM NaCl at room temperature for 10 hr. Size-exclusion chromatography was performed with a Pharmacia/LKB Superdex 75 10/30 column in 150 mM NaCl, 1 mM EDTA, 0.02% NaN_3, and either 25 mM PIPES (pH 7.4) or 50 mM sodium acetate (pH 5.5) on a Pharmacia/LKB FPLC system.

X-Ray Crystallography

Baculovirus-expressed, recombinant MIC-A was prepared and crystallized (space group $F4_132$, lattice constant a = b = c = 261.5 Å) as previously described (Bauer et al., 1998). There is one molecule per asymmetric unit resulting in a solvent content of approximately 80%. Data were collected at −170°C on either a Rigaku R-AXIS II or R-AXIS IV area detector with crystals cryo-preserved as previously described (Bauer et al., 1998). Diffraction data were processed with DENZO and scaled with SCALEPACK (Otwinowski and Minor, 1996). Using the Native(1) data, heavy atom positions in the $NaAuCl_4$ derivatives were determined by Patterson correlation search over the asymmetric unit with xhercules (McRee, 1993); all other heavy atom sites were located by difference Fourier syntheses. Initial phases (mean figure of merit = 0.63) were calculated with MLPHARE (Collaborative Computational Project, 1994). Initial phases were improved by solvent flattening and histogram matching using dm (Collaborative Computational Project, 1994) (Figure 1A). Models were built with O (Jones and Kjeldgaard, 1997). A total of 19 ordered solvent molecules were placed into $\geq 2\sigma$ peaks in difference Fourier syntheses with good hydrogen bond geometry. Initial positional refinement was performed with X-PLOR (Brünger, 1987) and subsequently with CNS (using the maximum likelihood target function mlf [Brünger et al., 1998]) against the Native(2) data. A bulk solvent correction (ksol = 0.3e/ Å^3, Bsol = 45 Å^2) and grouped B-factor refinement were applied in the later stages of refinement.

Acknowledgments

This work was supported in part by the Fred Hutchinson Cancer Research Center New Development Fund (R. K. S.), NIH grant AI30581 (T. S.) and a postdoctoral fellowship from the Deutsche Forschungsgemeinschaft (S. B.). We thank Barry Stoddard and Kam Zhang for advice during the crystallographic analysis.

Received February 22, 1999; revised April 15, 1999.

References

Allison, J.P., and Raulet, D.H. (1990). The immunobiology of $\gamma\delta$+ T cells. Semin. Immunol. *2*, 59–65.

Bahram, S., and Spies, T.A. (1996). Nucleotide sequence of a human *MHC* class I *MICB* cDNA. Immunogenetics *43*, 230–233.

Bahram, S., Bresnahan, M., Geraghty, D.E., and Spies, T.A. (1994). A second lineage of mammalian major histocompatibility complex class I genes. Proc. Natl. Acad. Sci. USA *91*, 6259–6263.

Bahram, S., Mizuki, N., Inoko, H., and Spies, T.A. (1996). Nucleotide sequence of the human MHC class I *MICA* gene. Immunogenetics *44*, 80–81.

Bauer, S., Willie, S.T., Spies, T., and Strong, R.K. (1998). Expression, purification, crystallization and crystallographic characterization of the human MHC class I related protein MICA. Acta Cryst. D. *54*, 451–453.

Bjorkman, P.J., and Parham, P. (1990). Structure, function and diversity of class I major histocompatibility complex molecules. Annu. Rev. Biochem. *90*, 253–88.

Brünger, A.T. (1987). X-PLOR Version 3.1. A System for X-ray Crystallography and NMR (New Haven and London: Yale University Press).

Brünger, A.T. (1992). Free R value: a novel statistical quantity for assessing the accuracy of crystal structures. Nature *355*, 472–475.

Brünger, A.T., Adams, P.D., Marius Clore, G., DeLano, W.L., Gros, P., Grosse-Kunstleve, R.W., Jiang, J.-S., Kuszewski, J., Nilges, M., Pannu, N.S., et al. (1998). Crystallography and NMR system: a new software suite for macromolecular structure determination. Acta Cryst. D. *54*, 905–921.

Burmeister, W.P., Gastinel, L.N., Simister, N.E., Blum, M.L., and Bjorkman, P.J. (1994a). Crystal structure at 2.2 Å resolution of the MHC-related neonatal Fc receptor. Nature *372*, 336–343.

Burmeister, W.P., Huber, A.H., and Bjorkman, P.J. (1994b). Crystal

structure of the complex of rat neonatal Fc receptor with Fc. Nature *372*, 379–383.

Chien, Y.H., and Jores, R. (1995). γδ T cells. T cells with B-cell-like recognition properties. Curr. Biol. *5*, 1116–1118.

Chien, Y.H., Jores, R., and Crowley, M.P. (1996). Recognition by γδ T cells. Annu. Rev. Immunol. *14*, 511–32.

Collaborative Computational Project, N. (1994). The CCP4 suite: programs for protein crystallography. Acta Cryst. D. *50*, 760–763.

Collins, E.J., Garboczi, D.N., Karpusas, M.N., and Wiley, D.C. (1995). The three-dimensional structure of a class I major histocompatibility complex molecule missing the α 3 domain of the heavy chain. Proc. Acad. Natl. Sci. USA *92*, 1218–1221.

Cosman, D., Fanger, N., Borges, L., Kubin, M., Chin, W., Peterson, L., and Hsu, M.L. (1997). A novel immunoglobulin superfamily receptor for cellular and viral MHC class I molecules. Immunity *7*, 273–282.

Davis, M.M., Boniface, J.J., Reich, Z., Lyons, D., Hampl, J., Arden, B., and Chien, Y. (1998). Ligand recognition by αβ T cell receptors. Annu. Rev. Immunol. *16*, 523–544.

Fahnestock, M.L., Johnson, J.L., Feldman, R.M.R., Neveu, J.M., Lane, W.S., and Bjorkman, P.J. (1995). The MHC class I homolog encoded by human cytomegalovirus binds endogenous peptides. Immunity *3*, 583–590.

Feder, J.N., Penny, D.M., Irrinki, A., Lee, V.K., Lebron, J.A., Watson, N., Tsuchihashi, Z., Sigal, E., Bjorkman, P.J., and Schatzman, R.C. (1998). The hemochromatosis gene product complexes with the transferrin receptor and lowers its affinity for ligand binding. Proc. Natl. Acad. Sci. USA *95*, 1472–1477.

Fodil, N., Laloux, L., Wanner, V., Pellet, P., Hauptmann, G., Mizuki, N., Inoko, H., Spies, T.A., Theodorou, I., and Bahram, S. (1996). Allelic repetoire of the human MHC class I *MICA* gene. Immunogenetics *44*, 351–357.

Germain, R.N., and Margulies, D.H. (1993). The biochemistry and cell biology of antigen processing and presentation. Annu. Rev. Immunol. *11*, 403–450.

Groh, V., Bahram, S., Bauer, S., Herman, A., Beauchamp, M., and Spies, T. (1996). Cell stress-regulated human major histocompatibility complex class I gene expressed in gastrointestinal epithelium. Proc. Natl. Acad. Sci. USA *93*, 12445–12450.

Groh, V., Steinle, A., Bauer, S., and Spies, T. (1998). Recognition of stress-induced MHC molecules by intestinal epithelial γδ T cells. Science *279*, 1737–1740.

Jones, T.A., and Kjeldgaard, M. (1997). Electron density map interpretation. Meth. Enzymol. *277*, 173–208.

Kaufmann, S.H. (1996). γδ and other unconventional T lymphocytes: what do they see and what do they do? Proc. Acad. Natl. Sci. USA *93*, 2272–2279.

Lebrón, J.A., Bennett, M.J., Vaughn, D.E., Chirino, A.J., Snow, P.M., Mintier, G.A., Feder, J.N., and Bjorkman, P.J. (1998). Crystal structure of the hemochromatosis protein HFE and characterization of its interaction with transferrin receptor. Cell *93*, 111–123.

McRee, D.E. (1993). Practical Protein Crystallography (San Diego: Academic Press, Inc.).

Nicholls, A., Sharp, K.A., and Honig, B. (1991). Protein folding and association: insights from the interfacial and thermodynamic properties of hydrocarbons. Proteins: Struct. Funct. Genet. *11*, 281–296.

Otwinowski, Z., and Minor, W. (1996). Processing of X-ray diffraction data collected in oscillation mode. Meth. Enzymol. *276*, 307–326.

Porcelli, S., Brenner, M.B., and Band, H. (1991). Biology of the human γδ T-cell receptor. Immunol. Rev. *120*, 137–183.

Porcelli, S.A., Segelke, B.W., Sugita, M., Wilson, I.A., and Brenner, M.B. (1998). The CD1 family of lipid antigen-presenting molecules. Immunol. Today *19*, 362–368.

Rammensee, H.-G., Falk, K., and Rötzschke, O. (1993a). MHC molecules as peptide receptors. Curr. Opin. Immunol. *5*, 35–44.

Rammensee, H.-G., Falk, K., and Rötzschke, O. (1993b). Peptides naturally presented by MHC class I molecules. Annu. Rev. Immunol. *11*, 213–244.

Rock, K.L. (1996). A new foreign policy: MHC class I molecules monitor the outside world. Immunol. Today *17*, 131–137.

Sanchez, L.M., Chirino, A.J., and Bjorkman, P.J. (1999). Crystal structure of human ZAG, a fat-depleting factor related to MHC molecules. Science *283*, 1914–1919.

Simister, N.E., and Rees, A.R. (1985). Isolation and characterization of an Fc receptor from neonatal rat small intestine. Eur. J. Immunol. *15*, 733–738.

Steinle, A., Groh, V., and Spies, T. (1998). Diversification, expression, and γδ T cell recognition of evolutionarily distant members of the MIC family of major histocompatibility complex class I-related molecules. Proc. Natl. Acad. Sci. USA *95*, 12510–12515.

Zeng, Z.-H., Castaño, A.R., Segelke, B.W., Stura, E.A., Peterson, P.A., and Wilson, I.A. (1997). Crystal structure of mouse CD1: an MHC-like fold with a large hydrophobic binding groove. Science *277*, 339–345.

Protein Data Bank ID Code

Coordinates for the 2.8 Å resolution MIC-A crystal sturcture (pH 5.5) have been deposited with the Protein Data Bank (code number 1b3j).